

Photochemically Generated Transients from κ^2 - and κ^3 -Triphos Derivatives of Group 6 Metal Carbonyls and Their Reactivity with Olefins

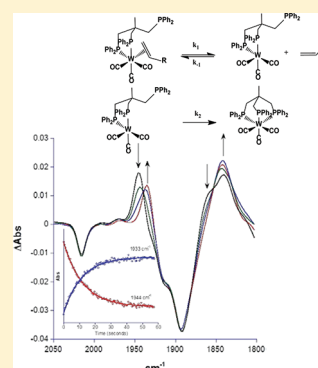
Samuel J. Kyran,[†] Sohail Muhammad,[‡] Matthew Knestrick,[†] Ashfaq A. Bengali,^{*,‡} and Donald J. Darensbourg^{*,†}

[†]Department of Chemistry, Texas A&M University, College Station, Texas 77843, United States

[‡]Department of Chemistry, Texas A&M University at Qatar, Doha, Qatar

S Supporting Information

ABSTRACT: The synthesis and characterization of $(\kappa^2\text{-Triphos})\text{M}(\text{CO})_4$ derivatives, where $\text{M} = \text{Mo}, \text{W}$ and $\text{Triphos} = \text{MeC}(\text{CH}_2\text{PPh}_2)_3$, are reported. Photolyses of these metal carbonyls in dichloromethane or CO_2 -saturated dichloromethane readily afford the $(\kappa^3\text{-Triphos})\text{M}(\text{CO})_3$ complexes with no evidence of significant solvent or carbon dioxide interactions with the site vacated by CO. However, in the presence of 1-hexene a transient $(\kappa^2\text{-Triphos})\text{M}(\text{CO})_3(1\text{-hexene})$ adduct was observed, which subsequently releases the olefin with formation of the stable κ^3 -tricarbonyl species. In the case of $\text{M} = \text{W}$ the kinetic parameters for this process were assessed, with the rate of olefin replacement being inversely proportional to $[1\text{-hexene}]$. A dissociative rate constant of $25.6 \pm 1.1 \text{ s}^{-1}$ at 298 K was determined for olefin loss, with the selectivity for 1-hexene vs free phosphine arm addition to the unsaturated intermediate being somewhat surprisingly large at 22. The activation parameters measured were $\Delta H^\ddagger = 26.1 \pm 0.4 \text{ kcal/mol}$ and $\Delta S^\ddagger = 36 \pm 3 \text{ eu}$, which are consistent with a dissociative substitution reaction. The kinetic parameters for this transformation were *unaffected* in the presence of excess quantities of CO_2 . Although no interaction of CO_2 with the transient species resulting from CO loss in the κ^2 complex was noted on the time scale of 50 ms, an intermediate described as an $\eta^2\text{-HSiEt}_3$ complex was observed upon addition of triethylsilane. This latter transient species underwent dissociation with κ^3 -complex formation about 15 times as fast as its 1-hexene analogue. X-ray structures of the κ^2 complexes of Mo and W where the dangling phosphine arm has undergone oxidation are also reported.

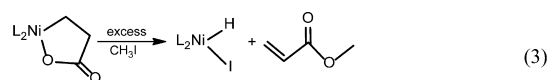
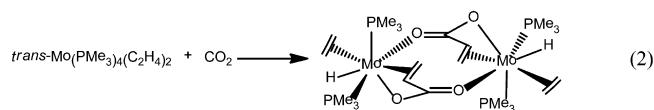
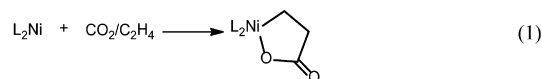


INTRODUCTION

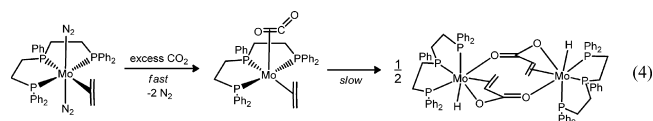
Alternative sources of chemical carbon for the production of fuels and useful organic chemicals will be required as the supply of petroleum declines during the current century. Carbon dioxide and biomass will serve as the major replacement feedstocks to fill this demand.¹ Relevant to this issue, the current major utilization of CO_2 in the chemical industry is the production of urea. Other less consuming applications involve the synthesis of salicylic acid, cyclic carbonates and polycarbonates, methanol, and inorganic carbonates.

Over the past decades we and numerous other research groups have investigated the alternating copolymerization of CO_2 and epoxides to provide polycarbonates.² Earlier we unsuccessfully studied the alternating coupling of CO_2 and olefins to provide polyesters. However, unlike the CO_2 /cyclic ether copolymerization process, this transformation is thermodynamically unfavorable except at low CO_2 incorporation.³ Nevertheless, there have been several investigations of CO_2 coupling with ethylene to provide either metallalactones⁴ or metal acrylate derivatives (eqs 1 and 2).⁵ Furthermore, promising reactions of metallalactones with methylating reagents to afford methyl acrylate have recently been reported (eq 3).⁶

Inspired by the kinetic and mechanistic studies reported by Bernskoetter and Tyler on the reaction of $(\text{Triphos})\text{Mo}(\text{N}_2)_2(\text{C}_2\text{H}_4)$,



Triphos = $(\text{Ph}_2\text{PCH}_2\text{CH}_2)_2\text{PPh}$, with CO_2 (eq 4), we wish to communicate herein some of our results covering the reactivity of phosphine derivatives of group 6 carbonyls with terminal olefins.⁷ Subsequent studies of these systems with carbon dioxide will also be described.



Received: January 19, 2012

Published: March 20, 2012



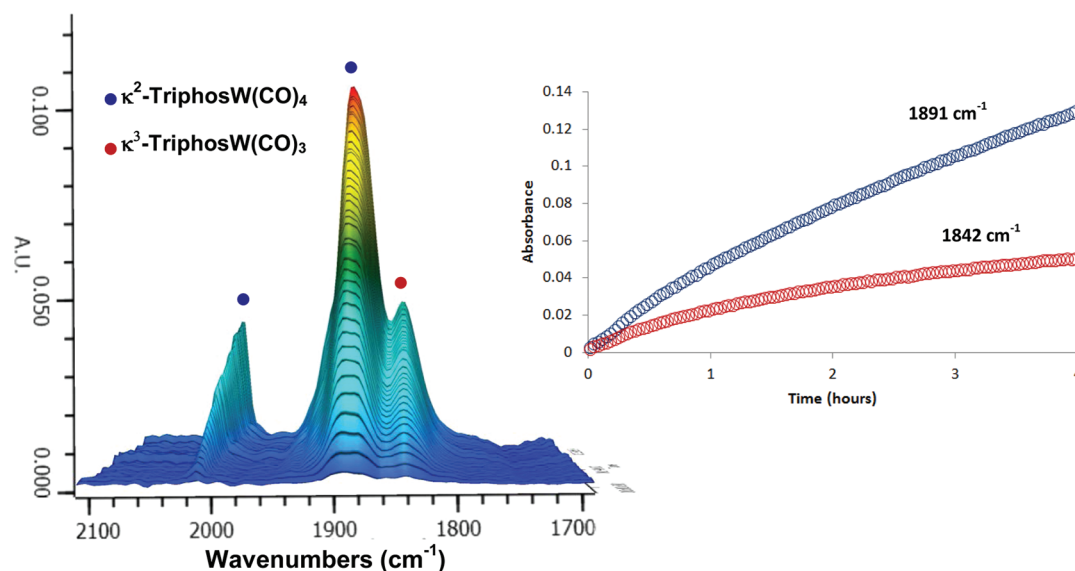


Figure 1. Three-dimensional stack plots (left) for the substitution reaction of *cis*-Mo(CO)₄(pip)₂ with Triphos in CHCl₃ at 308 K, where the starting material is subtracted out, and reaction profiles (right) for the formation of (κ^2 -Triphos)W(CO)₄ (1891 cm⁻¹) and (κ^3 -Triphos)W(CO)₃ (1842 cm⁻¹).

RESULTS AND DISCUSSION

Synthesis and Characterization. The reactions of *cis*-M(CO)₄(pip)₂ (M = Mo, W and pip = piperidine) with the tripodal version of Triphos, i.e., 1,1,1-tris(diphenylphosphinomethyl)ethane, provided κ^2 or κ^3 coordination, depending on reaction conditions. Although the κ^2 -Triphos derivatives of the group 6 tetracarbonyls have been prepared by direct substitution of the parent hexacarbonyl in refluxing ethanol,⁸ replacement of the labile piperidine ligands in *cis*-M(CO)₄(pip)₂ derivatives represents milder reaction conditions for the synthesis of κ^2 -[MeC(CH₂PPh₂)₃]M(CO)₄ complexes (M = Mo (**1a**), W (**1b**)).^{9,10} In a similar manner, when the reaction temperature and time were increased, the κ^3 -Triphos derivatives of molybdenum and tungsten tricarbonyls were formed. Interestingly, during the synthesis of the bidentate coordination of Triphos to either molybdenum or tungsten carbonyls under mild conditions, small quantities of the tridentate chelated ligand were observed. This was true in the short-term reactions carried out in refluxing dichloromethane (313 K) or over longer reaction times at ambient temperature. Figure 1 depicts the three-dimensional stack plots for the substitution reaction of *cis*-Mo(CO)₄(pip)₂ with Triphos in CHCl₃ at 308 K, along with the reaction profiles for the growth of κ^2 and κ^3 Mo carbonyl species. As is readily visible from the in situ infrared monitoring of the substitution reaction, formation of this κ^3 complex occurs concurrently with that of the κ^2 species, albeit at a slower rate. Further evidence for simultaneous formation of the κ^3 derivative is noted in the ³¹P NMR spectrum (see Figure 2). This behavior is suggestive of a phosphine-assisted (I_a) pathway for the displacement of CO in the κ^2 -Triphos complexes.¹¹ Support for such a process is noted from our observation that CO substitution in Mo(CO)₄(diphos) by PPh₃ takes place much more slowly by a dissociative mechanism.

The crystal structures of the (κ^3 -Triphos)M(CO)₃ (M = Mo (**2a**), W (**2b**)) complexes have been reported.¹² However, in all of our attempts at obtaining X-ray-quality crystals of the κ^2 -Triphos metal tetracarbonyls we obtained two crystalline forms, a cluster of needles and cubes; only the latter were suitable for

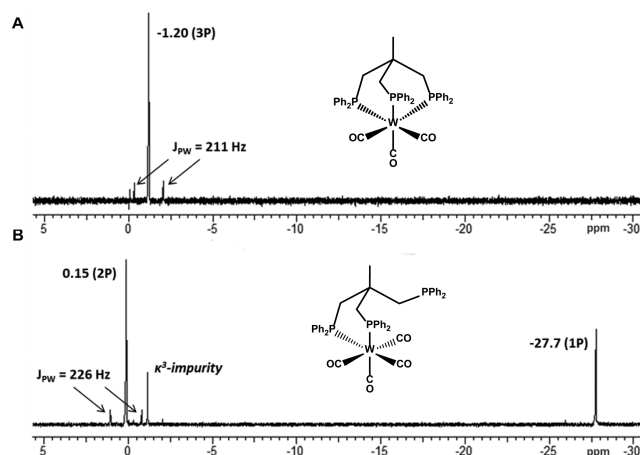


Figure 2. ³¹P NMR spectra: (A) purified sample of (κ^3 -Triphos)W(CO)₃; (B) isolated sample of (κ^2 -Triphos)W(CO)₄ from synthesis under mild conditions.

X-ray analysis. X-ray crystallography established these cube-shaped crystals to be the [(Ph₂PCH₂)₂CMeCH₂PPh₂(O)]M(CO)₄ (M = Mo (**3a**), W (**3b**)) complexes, where the free phosphine arm was oxidized despite all efforts to exclude oxygen and H₂O. ³¹P NMR revealed the mixture of crystals to be composed of approximately 80% of complex **3a** or **3b**, with the other unsuitable crystals for analysis being (κ^2 -Triphos)M(CO)₄. Previously, these derivatives have been synthesized by oxidation of the free phosphine arm in the κ^2 species with H₂O₂.¹⁰ The structures of these two metal complexes are shown in Figure 3. It is worth noting that PPh₃O has been shown to greatly aid the crystallization of organic materials and hence may account for the preferential well-defined crystals isolated of the oxidized form of the κ^2 species.¹³ Table 1 contains selected bond distances and angles for the two derivatives **3a,b**. The nonbonding distances between the phosphine oxide and the nearest CO ligand, O(5)⋯C(1), of 3.943(4) and 3.88(1) Å for the Mo and W derivatives, respectively, are greater than the sum of the van der Waals radii of 3.25 Å.

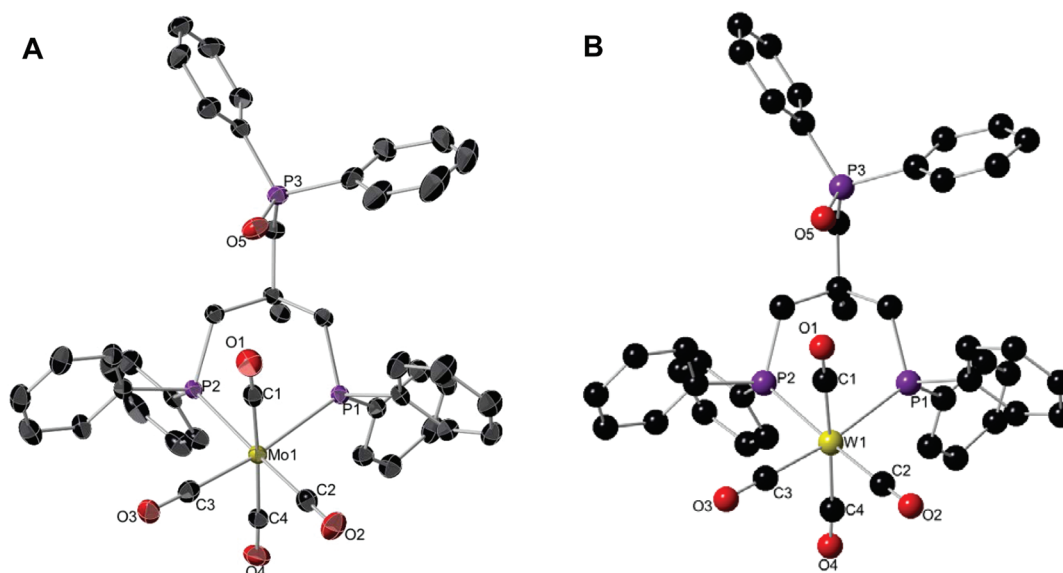


Figure 3. X-ray structures: (A) thermal ellipsoid representation of complex **3a** with ellipsoids at 50% probability surfaces (hydrogen atoms have been omitted for clarity); (B) ball-and-stick drawing of complex **3b**.

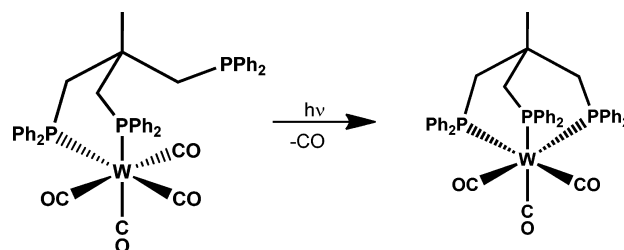
Table 1. Selected Bond Distances (Å) and Angles (deg) for Complexes **3a,b**

	M = Mo (3a)	M = W (3b)
M(1)–C(1)	2.020(3)	2.048(12)
M(1)–C(2)	1.999(3)	2.003(10)
M(1)–C(3)	2.001(3)	1.993(9)
M(1)–C(4)	2.054(3)	2.076(12)
M(1)–P(1)	2.5368(12)	2.529(3)
M(1)–P(2)	2.5041(12)	2.498(3)
O(5)–P(3)	1.483(2)	1.464(8)
C–O _{ave}	1.150(3)	1.139(12)
P(1)–M–P(2)	87.14(5)	87.11(9)
P(1)–M–C(1)	84.41(8)	84.3(3)
P(1)–M–C(2)	93.51(8)	93.2(3)
P(1)–M–C(3)	171.85(8)	170.8(3)
P(1)–M–C(4)	99.93(8)	99.8(3)
P(2)–M–C(1)	85.57(8)	84.8(3)
P(2)–M–C(2)	173.02(7)	173.2(3)
P(2)–M–C(3)	88.85(8)	89.1(2)
P(2)–M–C(4)	95.72(8)	96.4(3)

Kinetic Measurements. Kinetic studies designed to investigate the reactivity of terminal olefins with the Triphos derivatives of the group 6 metal carbonyls have been undertaken. Photolysis of a CH_2Cl_2 solution of $(\kappa^2\text{-Triphos})\text{W}(\text{CO})_4$ in the absence of 1-hexene resulted in the loss of a CO ligand, yielding only the $(\kappa^3\text{-Triphos})\text{W}(\text{CO})_3$ complex absorbing at 1933 and 1841 cm^{-1} , which has been isolated and characterized (Scheme 1).

It is well established that UV photolysis of metal carbonyls in the solution phase results in the photoejection of a CO ligand and solvent coordination to the vacant site occurs within picoseconds of CO loss.¹⁴ On the time scale of the present study, however (a few seconds), binding of CH_2Cl_2 to the W center upon photolysis is not observed. This finding is not surprising, since CH_2Cl_2 is expected to bind weakly to the W center and may undergo facile intramolecular displacement by the uncoordinated phosphine arm in the κ^2 structure.

Scheme 1



As shown in Figure 4, photolysis of $(\kappa^2\text{-Triphos})\text{W}(\text{CO})_4$ in the presence of 1-hexene results in spectral changes that are consistent with alkene coordination to the W center following CO loss. Upon photolysis, peaks are observed at 1944 and 1860 cm^{-1} which have band structures similar to those of the $(\kappa^3\text{-Triphos})\text{W}(\text{CO})_3$ complex, suggesting the formation of a transient tricarbonyl species. However, since the CO absorptions are blue-shifted (more electron poor metal center) relative to those of $(\kappa^3\text{-Triphos})\text{W}(\text{CO})_3$, it is reasonable to suggest that the third phosphine arm of the Triphos ligand remains uncoordinated in this intermediate complex.

This transient species undergoes a first-order exponential decay, and the $(\kappa^3\text{-Triphos})\text{W}(\text{CO})_3$ complex grows in at the same rate. The most likely candidate for this intermediate species is the $(\kappa^2\text{-Triphos})\text{W}(\text{CO})_3(\eta^2\text{-1-hexene})$ complex, which then undergoes intramolecular displacement of the 1-hexene ligand by the free phosphine arm of the Triphos ligand within a few seconds at room temperature. Further evidence for this assignment comes from the observation that the reaction rate varies inversely with [1-hexene]. As shown in Figure 5, an increase in [1-hexene] results in a slower displacement reaction, as evidenced by the longer lifetime of the $(\kappa^2\text{-Triphos})\text{W}(\text{CO})_3(\eta^2\text{-1-hexene})$ complex. The lifetime of the η^2 -alkene species is unaffected by increasing the concentration of the parent tetracarbonyl complex, thereby ruling out an intermolecular process in the displacement of the alkene.

A plot of k_{obs} obtained from a single-exponential fit to the observed decay of the η^2 -hexene complex, as a function of [1-hexene] is shown in Figure 6.

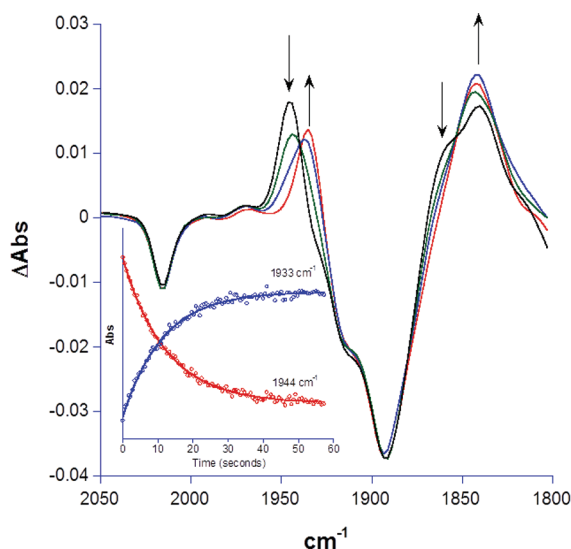


Figure 4. Spectral changes observed upon photolysis of $(\kappa^2\text{-Tripfos})\text{W}(\text{CO})_4$ in the presence of $[\text{1-hexene}] = 3.2 \text{ M}$ at 288 K. The peaks at 1944 and 1860 cm^{-1} assigned to the $(\kappa^2\text{-Tripfos})\text{W}(\text{CO})_3(\eta^2\text{-1-hexene})$ complex decrease in intensity, while those at 1933 cm^{-1} and 1841 cm^{-1} due to the $(\kappa^3\text{-Tripfos})\text{W}(\text{CO})_3$ complex grow at the same rate (see inset). The spectra were obtained 0, 5.8, 17.3, and 46.2 s after photolysis.

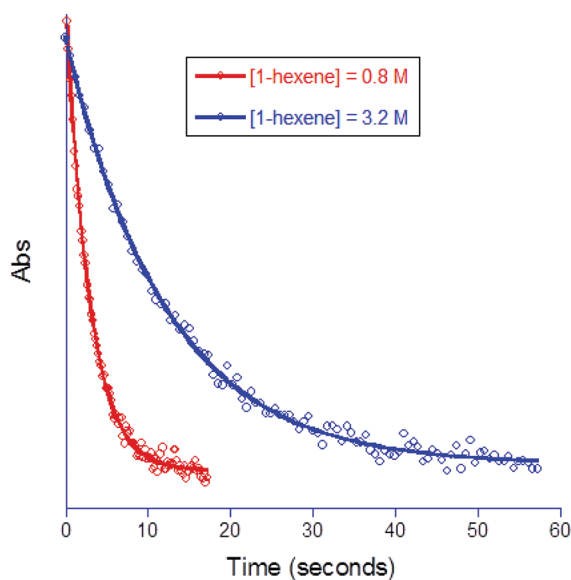


Figure 5. Effect of increasing 1-hexene concentration upon the decay rate of the $(\kappa^2\text{-Tripfos})\text{W}(\text{CO})_3(\eta^2\text{-1-hexene})$ complex at 288 K.

The inverse dependence of k_{obs} on $[\text{1-hexene}]$ is consistent with a displacement mechanism that involves reversible dissociation of the 1-hexene ligand prior to formation of the final $(\kappa^3\text{-Tripfos})\text{W}(\text{CO})_3$ product complex. A plausible mechanism is presented in Scheme 2.

Applying the steady state assumption to the 16-electron $(\kappa^2\text{-Tripfos})\text{W}(\text{CO})_3$ intermediate yields the following dependence of k_{obs} on $[\text{1-hexene}]$:

$$k_{\text{obs}} = \frac{k_1}{k'[\text{1-hexene}] + 1}, \text{ where } k' = \frac{k_{-1}}{k_2} \quad (5)$$

According to eq 5, limiting k_{obs} values of k_1 at low $[\text{1-hexene}]$ and 0 at high $[\text{1-hexene}]$ are expected if the above mechanism

is correct. Thus, at low $[\text{1-hexene}]$ the rate-determining step becomes the dissociation of the 1-hexene ligand, while the displacement rate approaches 0 at high $[\text{1-hexene}]$, as the

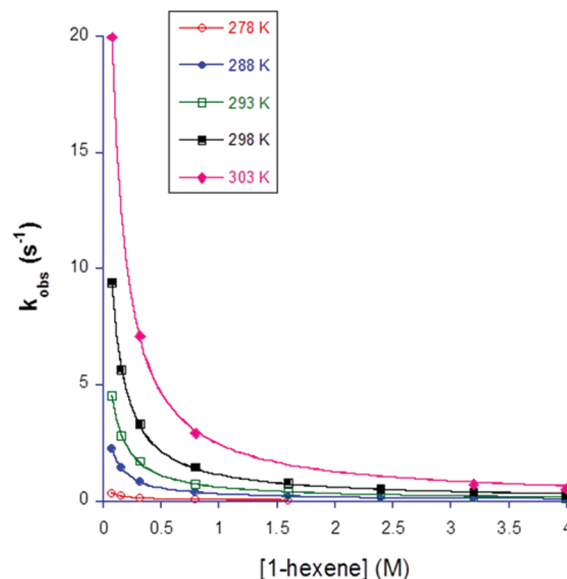


Figure 6. Plot of k_{obs} vs $[\text{1-hexene}]$ at various temperatures, illustrating the inverse dependence of k_{obs} on the concentration of 1-hexene.

presence of a large amount of free alkene inhibits the dissociation of the η^2 coordinated 1-hexene molecule. A fit of the experimental k_{obs} vs $[\text{1-hexene}]$ data to eq 5 yields values of k_1 and k' given in Table 2.

Surprisingly, the selectivity ratio k' is ~ 20 , which suggests that the 16-electron $(\kappa^2\text{-Tripfos})\text{W}(\text{CO})_3$ intermediate reacts faster with 1-hexene than with the phosphine arm of the Tripfos ligand. The temperature independence of k' further suggests that the enthalpic barriers for the reaction of $(\kappa^2\text{-Tripfos})\text{W}(\text{CO})_3$ with either 1-hexene or phosphine are similar or that they are both barrierless reactions. Previous studies have indicated that several 16-electron organometallic complexes react with a number of ligands without a significant enthalpic barrier, and so it is likely that this is the case in the present system as well.¹⁵ If so, then the kinetic preference of 1-hexene over intramolecular phosphine coordination may be due to entropic factors, although this is surprising, since ΔS^\ddagger_{-1} is expected to be considerably more negative than ΔS^\ddagger_2 . However, steric reorganization of the Tripfos ligand involved in $\kappa^2 \rightarrow \kappa^3$ coordination may result in a small barrier for the k_2 step. Given the relatively small temperature range over which the reactions were studied, the difference in ΔG^\ddagger for the two reactions may be as much as 2 kcal/mol, which could easily account for the observed selectivity ratio.

An Eyring plot obtained from the temperature dependence of k_1 , shown in Figure 7, yielded values of $\Delta H^\ddagger_1 = 26.1 \pm 0.4$ kcal/mol and $\Delta S^\ddagger_1 = 36 \pm 3$ eu. The strongly positive ΔS^\ddagger_1 is consistent with the dissociative nature of the transition state expected for the k_1 step, and ΔH^\ddagger_1 therefore provides an estimate for the $\text{W}-(\eta^2\text{-1-hexene})$ bond dissociation enthalpy (BDE). A BDE of 26.1 kcal/mol is consistent with an experimental determination of 24.8 kcal/mol for the $(\text{CO})_5\text{Cr}-(\eta^2\text{-C}_2\text{H}_4)$ BDE^{16–18} and a theoretical estimate of 26.2–28.9 kcal/mol for the $(\text{CO})_5\text{W}-(\eta^2\text{-C}_2\text{H}_4)$ BDE.^{19,20}

Scheme 2

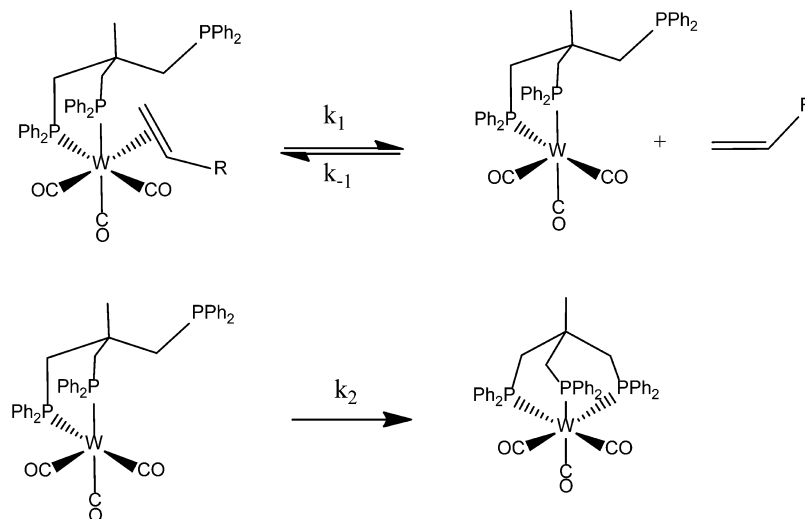


Table 2. Kinetic Parameters Obtained from a Fit of the k_{obs} vs [1-hexene] Data to Eq 5^a

T (K)	k_1 (s^{-1})	k' ($=k_{-1}/k_2$)
278	0.96 ± 0.04	24 ± 1
288	5.3 ± 0.2	17 ± 1
293	10.8 ± 0.5	18 ± 1
298	25.6 ± 1.1	22 ± 1
303	52.5 ± 3	21 ± 2

^aRate constants were obtained using KaleidaGraph version 4.1.0, Synergy Software, Reading, PA, USA. The R^2 values for the fits at various temperatures were all greater than 0.999.

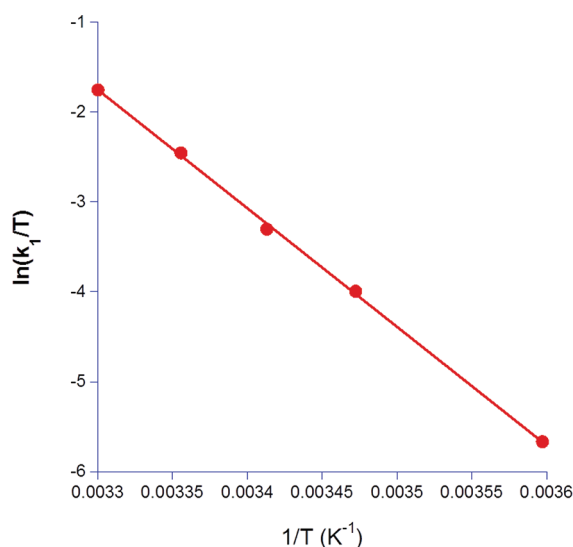


Figure 7. Eyring plot obtained from the temperature dependence of k_1 . The equation for the trend line was $y = 41.776 - 13190x$, with an R^2 value of 0.9993.

A few experiments were conducted with the analogous Mo system, and as shown in Figure 8, it was found that under similar conditions of temperature and [1-hexene], the $(\kappa^2\text{-Triphos})\text{Mo}(\text{CO})_3(\eta^2\text{-1-hexene})$ reacted almost 200 times faster than the W complex. This is perhaps not surprising, since the $\text{Mo}-(\eta^2\text{-1-hexene})$ BDE is expected to be weaker than that in the W system. Thus, for example, the calculated $(\text{CO})_5\text{M}-$

$(\eta^2\text{-C}_2\text{H}_4)$ BDE is almost 4 kcal/mol less for $\text{M} = \text{Mo}$ than for $\text{M} = \text{W}$.^{19,20}

Of particular interest in this study are photochemical reactions of $(\kappa^2\text{-Triphos})\text{W}(\text{CO})_4$ in the presence of excess quantities of carbon dioxide. As is evident in Figure 9A from the difference spectrum obtained upon photolysis of a CO_2 -saturated solution of $(\kappa^2\text{-Triphos})\text{W}(\text{CO})_4$ in dichloromethane at 296 K, only $(\kappa^3\text{-Triphos})\text{W}(\text{CO})_3$ is observed. This observation suggests that either CO_2 does not bind to the vacant site or that it binds weakly, resulting in a transient species that has a lifetime that is too short to detect on this time scale (<50 ms). Similarly, the difference spectra obtained upon photolysis of a CO_2 -saturated solution of $(\kappa^2\text{-Triphos})\text{W}(\text{CO})_4$ in CH_2Cl_2 with [1-hexene] = 1.6 M at 298 K revealed spectral characteristics and reaction rate constants identical with those of the process determined in the absence of CO_2 (Figure 9B).²¹ Taken together, these results strongly support the lack of significant CO_2 interactions with the vacant site in $(\kappa^2\text{-Triphos})\text{W}(\text{CO})_3$, especially in comparison with the corresponding binding of an olefin ligand.

By way of contrast, a rather strong interaction is observed between triethylsilane and the transient tricarbonyl species afforded upon photolysis of $(\kappa^2\text{-Triphos})\text{W}(\text{CO})_4$. This is illustrated in Figure 10, where the two $(\kappa^2\text{-Triphos})\text{W}(\text{CO})_3\text{-(silane)}$ ν_{CO} bands are similar to those seen in the 1-hexene analogue, although as expected these are red-shifted by 5–8 cm^{-1} . However, the initial species reacts with the free phosphine arm to afford $(\kappa^3\text{-Triphos})\text{W}(\text{CO})_3$ almost 15 times more quickly than the 1-hexene complex. Given the position of the ν_{CO} bands in the intermediate and its reactivity, this species is most likely $(\kappa^2\text{-Triphos})\text{W}(\text{CO})_3(\eta^2\text{-HSiEt}_3)$ and not a Si–H activated complex.

Preliminary results on the interactions of 1-hexene in $(\kappa^2\text{-Triphos})\text{W}(\text{CO})_3(1\text{-hexene})$ and $(\kappa^3\text{-Triphos})\text{W}(\text{CO})_2(1\text{-hexene})$ reveal olefin binding in these complexes to be quite similar: i.e., the lifetimes of the two hexene complexes are comparable. Further studies to examine these interactions as well as the binding of olefins with metal carbonyl transients photochemically generated from more electron-rich precursors in the presence and absence of CO_2 are planned.

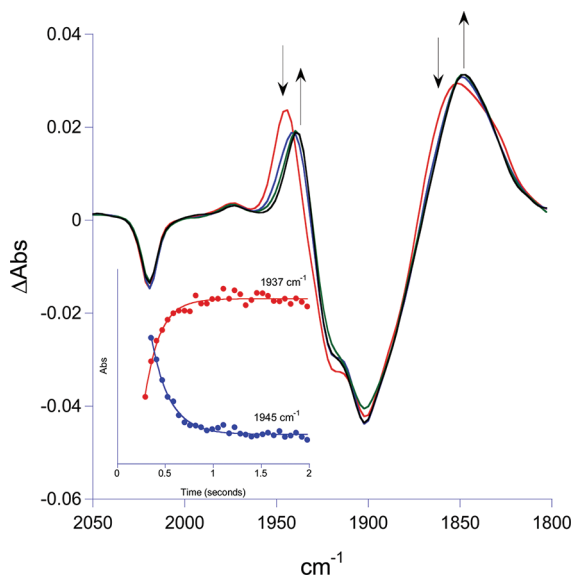


Figure 8. Spectral changes observed upon photolysis of $(\kappa^2\text{-Triphos})\text{Mo}(\text{CO})_4$ in the presence of $[1\text{-hexene}] = 2.4\text{ M}$ at 278 K.

CONCLUDING REMARKS

We have shown herein that photolysis of $(\kappa^2\text{-Triphos})\text{W}(\text{CO})_4$ in the presence of 1-hexene affords a short-lived $(\kappa^2\text{-Triphos})\text{-W}(\text{CO})_3(1\text{-hexene})$ complex which subsequently undergoes loss of the olefin with concomitant formation of the stable $(\kappa^3\text{-Triphos})\text{W}(\text{CO})_3$ derivative. The transient 1-hexene adduct was found to sustain intramolecular displacement of the olefin ligand by the free phosphine arm with a reaction rate which varied inversely with $[1\text{-hexene}]$, indicative of a dissociative process. Furthermore, the unsaturated intermediate was shown to be ~ 20 times more selective for olefin coordination as compared to the uncoordinated phosphine. The molybdenum analogue was shown to undergo these transformations on a

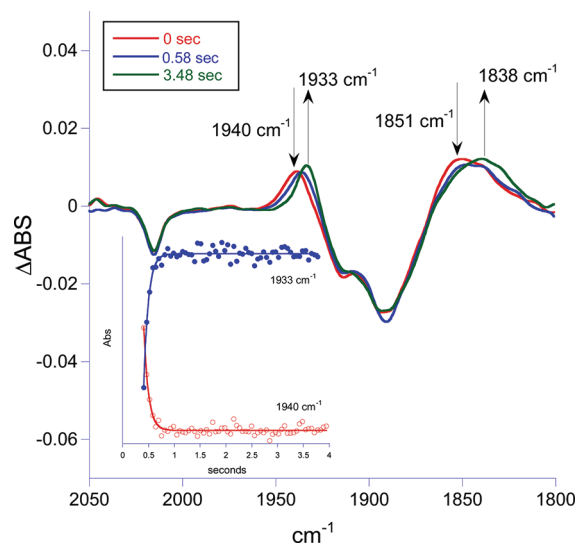


Figure 10. Difference spectra obtained upon photolysis of a CH_2Cl_2 solution of $(\kappa^2\text{-Triphos})\text{W}(\text{CO})_4$ with $[\text{HSiEt}_3] = 1.25\text{ M}$ at 288 K.

much shorter time scale. The activation parameters for the replacement of the 1-hexene ligand in the tungsten complex were determined to be $\Delta H^\ddagger = 26.1\text{ kcal/mol}$ and $\Delta S^\ddagger = 36\text{ eu}$. The enthalpy of activation closely relates to the estimated value of the BDE, as expected for a dissociative reaction. Attempts to observe a CO_2 adduct with the transient provided by photolysis of $(\kappa^2\text{-Triphos})\text{W}(\text{CO})_4$ were unsuccessful, indicative of no binding or weak binding with a lifetime of binding less than 10^{-3} s . Similarly, the kinetic parameters for 1-hexene binding were unaffected by the presence of excess quantities of CO_2 in solution. That is, CO_2 coordination at the vacant metal site is not competitive with olefin binding. On the other hand, the transient complex $(\kappa^2\text{-Triphos})\text{W}(\text{CO})_3(\text{HSiEt}_3)$ was observed upon photolysis of $(\kappa^2\text{-Triphos})\text{W}(\text{CO})_4$ in the presence of

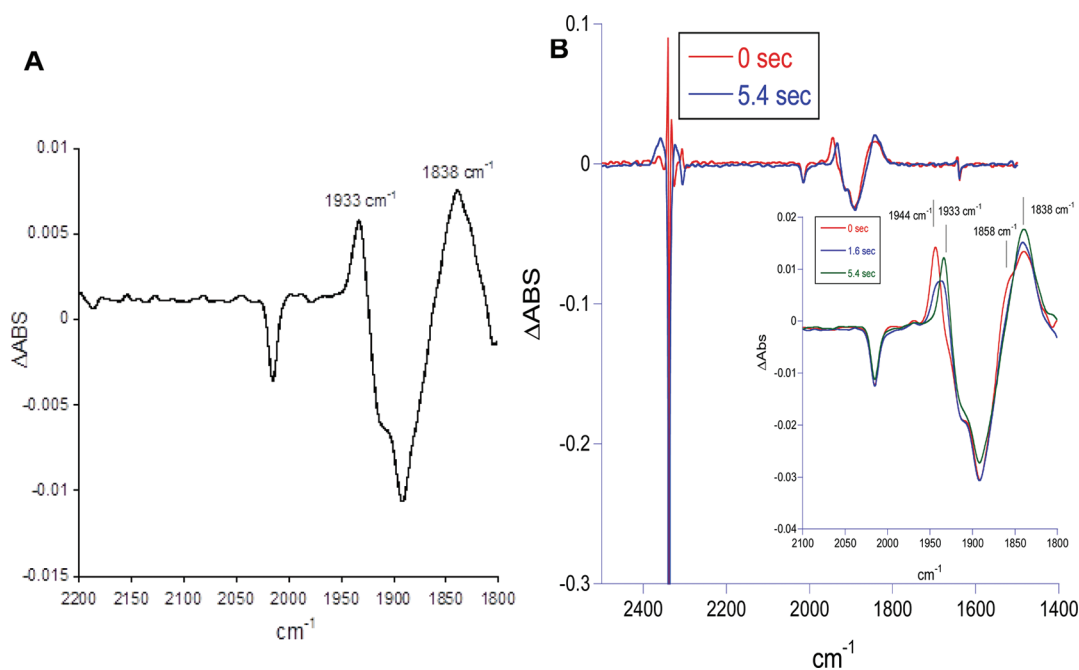


Figure 9. (A) Difference spectrum obtained upon photolysis of a CO_2 -saturated solution of $(\kappa^2\text{-Triphos})\text{W}(\text{CO})_4$ in CH_2Cl_2 at 296 K. (B) Difference spectra obtained upon photolysis of a CO_2 -saturated solution of $(\kappa^2\text{-Triphos})\text{W}(\text{CO})_4$ in the presence of 1.6 M 1-hexene at 298 K. The strong band in the $2330\text{--}2350\text{ cm}^{-1}$ region is due to CO_2 .

triethylsilane at ambient temperature. On the basis of the ν_{CO} bands in the HSiEt_3 adduct and its rapid dissociation, about 15 times more labile than 1-hexene, this species is assumed to be $(\kappa^2\text{-Triphos})\text{W}(\text{CO})_3(\eta^2\text{-HSiEt}_3)$.

EXPERIMENTAL SECTION

Methods and Materials. All reactions were carried out under an argon atmosphere. Dichloromethane was purified by an MBraun Manual Solvent Purification System packed with Alcoa F200 activated alumina desiccant. Decalin (Aldrich) was degassed before use. Methanol and chloroform were used as purchased from EMD chemicals. The ligand 1,1,1-tris(diphenylphosphinomethyl)ethane (Triphos) was purchased from Sigma-Aldrich, and the metal–carbonyl precursors $\text{M}(\text{CO})_4(\text{pip})_2$ ($\text{M} = \text{Mo}, \text{W}$) were prepared as per the literature.⁹ NMR spectra were recorded on a Varian INOVA 300 (operating at 299.96 and 121.43 MHz for ^1H and ^{31}P , respectively) and Varian MERCURY 300 (operating at 75.42 MHz for ^{13}C) spectrometers. ^1H and ^{13}C NMR spectra were referenced to residual solvent resonances, while ^{31}P NMR spectra were referenced to an external H_3PO_4 in D_2O at 0.0 ppm. Infrared spectra were obtained on a Bruker Tensor 27 FTIR spectrometer. In situ IR monitoring was carried out using a Mettler Toledo iC10 ReactIR with an AgX fiber conduit probe. Elemental analyses were determined by Atlantic Microlab (Norcross, GA).

Synthesis of $(\kappa^2\text{-Triphos})\text{Mo}(\text{CO})_4$. $\text{Mo}(\text{CO})_4(\text{pip})_2$ (0.894 g, 2.36 mmol) and Triphos (1.500 g, 2.40 mmol) in dichloromethane (100 mL) were heated to reflux for 30 min. The resulting orange solution was filtered through Celite, and the filtrate was reduced in volume to ca. 5 mL and treated with methanol to give a tan precipitate. Recrystallization from chloroform/methanol yielded a white product (1.550 g, 79%). IR data in CH_2Cl_2 (ν_{CO}): 1870 (sh), 1901 (s), 1920 (sh), 2020 (m). NMR data in CDCl_3 : $^{31}\text{P}\{^1\text{H}\}$ δ -27.7 (t, $J_{\text{P-P}} = 2$, 1 P), 19.7 (d, $J_{\text{P-P}} = 2$, 2 P); ^1H δ 0.75 (s, 3 H, CH_3), 2.15 (m, 2 H, CH_2), 2.43 (dd, $^2J_{\text{H-H}} = 14$, $^2J_{\text{H-P}} = 4$, 2 H, CH_2), 2.71 (dd, $^2J_{\text{H-H}} = 14$, $^2J_{\text{H-P}} = 9$, 2 H, CH_2), 7.25–7.46 (m, 26 H, C_6H_5), 7.60–7.70 (m, 4 H, C_6H_5); selected $^{13}\text{C}\{^1\text{H}\}$ δ 209.6 (t, $^2J_{\text{C-P}} = 8$, 1 C, CO), 211.1 (t, $^2J_{\text{C-P}} = 9$, 1 C, CO), 215.3 (m, 2 C, *trans*-CO). Anal. Calcd for $\text{C}_{45}\text{H}_{39}\text{MoO}_4\text{P}_3$: C, 64.9; H, 4.7. Found: C, 64.4; H, 4.6.

Synthesis of $(\kappa^2\text{-Triphos})\text{Mo}(\text{CO})_3$. $\text{Mo}(\text{CO})_4(\text{pip})_2$ (0.897 g, 2.37 mmol) and Triphos (1.504 g, 2.41 mmol) in decalin (110 mL) were heated to reflux for 19 h. The resulting brown solid was isolated by filtration and washed with methanol until the filtrate ran clear. Recrystallization from chloroform/methanol yielded a white product (1.410 g, 74%). IR data in CH_2Cl_2 (ν_{CO}): 1844 (s), 1938 (s). NMR data in CDCl_3 : $^{31}\text{P}\{^1\text{H}\}$ δ 18.2 (s, 3 P); ^1H δ 1.44 (m, 3 H, CH_3), 2.26 (m, 6 H, CH_2), 7.08 (t, $^3J_{\text{H-H}} = 7.2$, 12 H, H_m), 7.18 (t, $^3J_{\text{H-H}} = 7.2$, 6 H, H_p), 7.35 (m, 12 H, H_o); ^{13}C NMR data could not be obtained due to low solubility of the compound. Anal. Calcd for $\text{C}_{44}\text{H}_{39}\text{MoO}_3\text{P}_3$: C, 65.7; H, 4.9. Found: C, 65.5; H, 4.7.

Synthesis of $(\kappa^2\text{-Triphos})\text{W}(\text{CO})_4$. $\text{W}(\text{CO})_4(\text{pip})_2$ (0.700 g, 1.50 mmol) and Triphos (1.000 g, 1.60 mmol) in dichloromethane (100 mL) were heated to reflux for 4 h. The resulting clear yellow solution was reduced in volume to ca. 5 mL and treated with methanol to give a yellow precipitate. Recrystallization from chloroform/methanol yielded a pale yellow product (0.597 g, 43%). IR data in CH_2Cl_2 (ν_{CO}): 1861 (sh), 1892 (s), 1915 (sh), 2011 (m). NMR data in CDCl_3 : $^{31}\text{P}\{^1\text{H}\}$ δ -27.7 (t, $J_{\text{P-P}} = 2$, 1 P), 0.15 (d, $J_{\text{P-P}} = 2$ ($J_{\text{P-W}} = 226$, satellite), 2 P); ^1H δ 0.76 (s, 3 H, CH_3), 2.13 (m, 2 H, CH_2), 2.52 (dd, $^2J_{\text{H-H}} = 14$, $^2J_{\text{H-P}} = 5$, 2 H, CH_2), 2.81 (dd, $^2J_{\text{H-H}} = 14$, $^2J_{\text{H-P}} = 10$, 2 H, CH_2), 7.27–7.45 (m, 26 H, C_6H_5), 7.58–7.68 (m, 4 H, C_6H_5); selected $^{13}\text{C}\{^1\text{H}\}$ δ 202.1 (t, $^2J_{\text{C-P}} = 7$, 1 C, CO), 203.5 (t, $^2J_{\text{C-P}} = 7$, 1 C, CO), 206.0 (m, 2 C, *trans*-CO). Anal. Calcd for $\text{C}_{45}\text{H}_{39}\text{W}_4\text{O}_4\text{P}_3$: C, 58.7; H, 4.3. Found: C, 58.1; H, 4.2.

Synthesis of $(\kappa^3\text{-Triphos})\text{W}(\text{CO})_3$. $\text{W}(\text{CO})_4(\text{pip})_2$ (1.101 g, 2.36 mmol) and Triphos (1.504 g, 2.41 mmol) in decalin (100 mL) were heated to reflux for 20 h. The resulting gray solid was isolated by filtration and washed with ether (2×25 mL). Recrystallization from chloroform/methanol twice yielded a white product (0.874 g, 42%). IR data in CH_2Cl_2 (ν_{CO}): 1841 (s), 1933 (s). NMR data in CDCl_3 :

$^{31}\text{P}\{^1\text{H}\}$ δ -1.4 (s, $J_{\text{P-W}} = 211$ (satellite), 3 P); ^1H δ 1.43 (m, 3 H, CH_3), 2.35 (m, 6 H, CH_2), 7.09 (t, $^3J_{\text{H-H}} = 7.2$, 12 H, H_m), 7.18 (t, $^3J_{\text{H-H}} = 7.2$, 6 H, H_p), 7.34 (m, 12 H, H_o); ^{13}C NMR data could not be obtained due to low solubility of the compound. Anal. Calcd for $\text{C}_{44}\text{H}_{39}\text{O}_3\text{P}_3\text{W}$: C, 59.2; H, 4.4. Found: C, 59.0; H, 4.3.

Kinetic Measurements. In a typical experiment, the photolysis solution was ~ 4 mM in $(\kappa^2\text{-Triphos})\text{W}(\text{CO})_4$ dissolved in dichloromethane with varying amounts of 1-hexene. The reactions were conducted over a 25 K temperature range from 278 to 303 K, and the 1-hexene concentration was varied over a 50-fold range (0.08–4 M). A Bruker Vertex 80 FTIR equipped with both step-scan and rapid-scan capabilities was used to obtain the IR spectra using a temperature-controlled 0.75 mm path length transmission cell with CaF_2 windows. Spectra were obtained at 8 cm^{-1} resolution. Photolysis was conducted with 355 nm light from a Nd:YAG laser (Continuum Surelite I-10). Spectral acquisition was initiated following a single shot of the UV laser (30 mJ/pulse), which was collinear with the IR beam and defocused to ensure irradiation of the entire cell volume.

ASSOCIATED CONTENT

Supporting Information

CIF files giving X-ray structural data for **3a,b**. This material is available free of charge via the Internet at <http://pubs.acs.org>.

AUTHOR INFORMATION

Notes

The authors declare no competing financial interest.

ACKNOWLEDGMENTS

This publication was made possible by NPRP Grant No. 09-157-1-024 from the Qatar National Research Fund (a member of Qatar Foundation). The statements made herein are solely the responsibility of the authors. M. K. was a participant in the NSF REU Program (No. CHE-1062840) at College Station, TX.

REFERENCES

- (1) (a) Aresta, M. In *Carbon Dioxide as Chemical Feedstock*; Aresta, M., Ed.; Wiley-VCH: Weinheim, Germany, 2010. (b) Mathers, R. T. *J. Polym. Sci., Part A: Polym. Chem.* **2012**, *50*, 1.
- (2) For reviews in this area, see: (a) Coates, G. W.; Moore, D. R. *Angew. Chem., Int. Ed.* **2004**, *43*, 6618. (b) Darensbourg, D. J.; Mackiewicz, R. M.; Phelps, A. L.; Billodeaux, D. R. *Acc. Chem. Res.* **2004**, *37*, 836. (c) Darensbourg, D. J. *Chem. Rev.* **2007**, *107*, 2388. (d) Sugimoto, H.; Inoue, S. *J. Polym. Sci., Part A: Polym. Chem.* **2004**, *42*, 5561. (e) Kember, M. R.; Buchard, A.; Williams, C. K. *Chem. Commun.* **2011**, 141. (f) Klaus, S.; Lehenmeier, M. W.; Anderson, C. E.; Rieger, B. *Coord. Chem. Rev.* **2011**, *255*, 1460.
- (3) Price, C. J.; Reich, B. J. E.; Miller, S. A. *Macromolecules* **2006**, *39*, 2751.
- (4) (a) Hoberg, H.; Schaefer, D. J. *Organomet. Chem.* **1982**, *236*, C28. (b) Hoberg, H.; Schaefer, D. J. *Organomet. Chem.* **1983**, *251*, C51. (c) Walther, D.; Dinjus, E.; Sieler, J.; Anderson, L.; Lindqvist, O. *J. Organomet. Chem.* **1984**, *276*, 99. (d) Walter, D.; Bräunlich, G.; Kempe, R.; Sieler, J. *J. Organomet. Chem.* **1992**, *436*, 109.
- (5) (a) Alvarez, R.; Carmona, E.; Colc-Hamilton, D. J.; Galindo, A.; Gutierrez-Puebla, E.; Monge, A.; Poveda, M. L.; Ruiz, C. *J. Am. Chem. Soc.* **1985**, *107*, 5529. (b) Alvarez, R.; Carmona, E.; Galindo, A.; Gutierrez, E.; Marin, J. M.; Monge, A.; Poveda, M. L.; Ruiz, C.; Savariault, J. M. *Organometallics* **1989**, *8*, 2430. (c) Galindo, A.; Pastor, A.; Perez, P.; Carmona, E. *Organometallics* **1993**, *12*, 4443.
- (6) Lee, S. Y. T.; Cokoja, M.; Drees, M.; Li, Y.; Mink, J.; Herrmann, W. A.; Kuhn, F. E. *ChemSusChem* **2011**, *4*, 1275.
- (7) Bernskoetter, W. H.; Tyler, B. T. *Organometallics* **2011**, *30*, 520.
- (8) Chatt, J.; Leigh, G. J.; Thankarajan, N. *J. Organomet. Chem.* **1971**, *29*, 105.
- (9) Darensbourg, D. J.; Kump, R. L. *Inorg. Chem.* **1978**, *17*, 2680.

- (10) Fernandez, E. J.; Gimeno, M. C.; Jones, P. G.; Laguna, A.; Laguna, M.; Olmos, E. *J. Chem. Soc., Dalton Trans.* **1996**, 3603.
- (11) (a) Keiter, R. L.; Ye, P.; Keiter, E. A.; Benson, J. W.; Lin, W.; Brandt, D. E.; Southern, J. S.; Rheingold, A. L.; Guzei, I.; Wheeler, K. A.; Cary, L. W. *Inorg. Chim. Acta* **2010**, 364, 176. (b) Darensbourg, D. J.; Wiegrefe, H. P. *Inorg. Chem.* **1990**, 29, 592. (c) Darensbourg, D. J.; Joyce, J. A.; Bischoff, C. J.; Reibenspies, J. H. *Inorg. Chem.* **1991**, 30, 1137.
- (12) (a) Walter, Q.; Klein, T.; Huttner, G.; Zsolnai, L. *J. Organomet. Chem.* **1993**, 458, 63. (b) Dilsky, S. *J. Organomet. Chem.* **2007**, 692, 2887.
- (13) Etter, M. C.; Baures, P. W. *J. Am. Chem. Soc.* **1988**, 110, 639.
- (14) (a) Lee, M.; Harris, C. B. *J. Am. Chem. Soc.* **1989**, 111, 8963. (b) Yu, S. C.; Xu, X.; Lingle, R. Jr.; Hopkins, J. B. *J. Am. Chem. Soc.* **1990**, 112, 3668. (c) Joly, A. G.; Nelson, K. A. *Chem. Phys.* **1991**, 152, 69. (d) Hall, C.; Perutz, R. N. *Chem. Rev.* **1996**, 3125. (e) Xie, X.; Simon, J. D. *J. Am. Chem. Soc.* **1990**, 112, 1130.
- (15) Zheng, Y.; Wang, W.; Lin, J.; She, Y.; Fu, K.-J. *J. Phys. Chem.* **1992**, 96, 7650.
- (16) An average value from the references in ref 15.
- (17) (a) McNamara, B.; Becher, D. M.; Towns, M. H.; Grant, E. R. *J. Phys. Chem.* **1994**, 98, 4622. (b) McNamara, B.; Towns, M. H.; Grant, E. R. *J. Am. Chem. Soc.* **1995**, 117, 12254. (c) Wells, J. R.; House, P. G.; Weitz, E. *J. Phys. Chem.* **1994**, 98, 11256.
- (18) Cedeño, D. L.; Weitz, E. *J. Am. Chem. Soc.* **2001**, 123, 12857.
- (19) Schlappi, D. N.; Cedeño, D. L. *J. Phys. Chem. A* **2009**, 113, 9692.
- (20) Cedeño, D. L.; Sniatynsky, R. *Organometallics* **2005**, 24, 3882.
- (21) It is important to note here that this experiment involves complex **1b** leading to **2b** plus CO upon photolysis in the presence of CO₂ and does not involve the uncoordinating phosphine oxide complex **3b**.